ELSEVIER

Physics Letters B 527 (2002) 50–54

PHYSICS LETTERS B

www.elsevier.com/locate/npe

First observation of neutron–proton halo structure for the 3.563 MeV 0^+ state in ^{6}Li via ^{1}H(^{6}He, ^{6}Li)n reaction

Zhihong Li, Weiping Liu, Xixiang Bai, Youbao Wang, Gang Lian, Zhichang Li, Sheng Zeng

China Institute of Atomic Energy, P.O. Box 275(46), Beijing 102413, PR China

Received 15 October 2001; received in revised form 3 December 2001; accepted 21 December 2001

Editor: V. Metag

Abstract

The angular distributions of the charge exchange reaction ^{1}H(^{6}He, ^{6}Li)n were measured in reverse kinematics with a secondary ^{6}He beam at the energy of 4.17 A MeV. The data were analyzed in the context of a microscopic calculation. It is shown that both the ground state of ^{6}He and the second excited state of ^{6}Li (3.563 MeV, 0^+) have halo structure.

PACS: 21.10.-k; 21.10.Ft; 21.10.Gv; 25.60.Lg

Keywords: ^{1}H(^{6}He, ^{6}Li)n reaction in inverse kinematics; Angular distribution; Microscopic optical potential; Nucleon density distribution; Proton–neutron halo structure

So far the prominent halo structure has been revealed in the ground states of some nuclei near the neutron drip line. As the nuclei near the neutron drip line have high isospin, Y. Suzuki et al. [1] raised a question: "What about the possibility that stable nuclei have extended halolike structure in high isospin excited states?" If the answer is positive, the isobaric analog state (IAS) of the neutron halo nuclei should also have halolike structure. Arai et al. [2] calculated the nucleon density distributions of the ground state of ^{6}He and of its isobaric analog state, i. e., the 3.563 MeV 0^+ state of ^{6}Li with a fully microscopic three-cluster model and predicted that the latter has a more conspicuous halolike structure formed by the neutron and the proton surrounding the α core as compared to the former.

In recent years, the ^{1}H(^{6}He, ^{6}Li)n charge exchange reaction has been studied experimentally by two groups at beam energies of 93 A MeV and 41.6 A MeV, respectively [3–6]. The aim of these experiments was in search for the signature of halo structure through the measurement of the angular distributions at very forward angles for the Gamow–Teller transition to the ground state of ^{6}Li and for the Fermi transition to the 3.563 MeV 0^+ state of ^{6}Li. No signature of halo structure was found in these experiments, however. A microscopic analysis indicated that the presence or absence of a halo structure would not influence the transition strength at 0° [5]. The halo ef-

E-mail address: zhli@iris.ciae.ac.cn (Z. Li).

0370-2693/02/$ – see front matter
PII: S0370-2693(02)01172-3

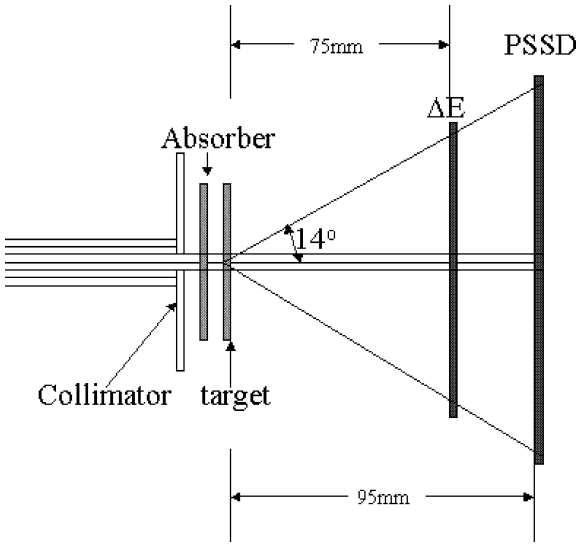

Fig. 1. Experimental setup.

fect should appear in the region of large angles. Thus the measurement of full angular distributions for the ^{1}H(^{6}He, ^{6}Li)n reaction is necessary.

In this Letter, we briefly report our experiment of the ^{1}H(^{6}He, ^{6}Li)n reaction in reverse kinematics with a secondary ^{6}He beam at the energy of 4.17 A MeV and a microscopic analysis.

The experiment was carried out using the secondary beam facility [7] of the HI-13 tandem accelerator at China Institute of Atomic Energy, Beijing. The experimental setup was similar to the previously illustrated [8], as shown in Fig. 1. A ^{7}Li beam with energy of 44 MeV from the tandem impinged on a D_2 gas cell at pressure of 1.5 atm, in which ^{6}He ions were produced via ^{2}H(^{7}Li, ^{6}He)^{3}He reaction. The front and rear windows of the gas cell were Havar foils, each in thickness of 1.9 mg/cm^2. The ^{6}He beam with energy of 35.7 MeV was delivered through a careful tuning of the magnets' currents. The typical purity of ^{6}He beam was about 90%. The main contaminants were ^{7}Li^{2+}, ^{7}Li^{3+}, ^{4}He^{2+} and ^{6}Li^{2+} ions. Because the reaction products to be detected were the ^{6}Li ions, the ^{6}Li^{2+} contaminants would make a severe disruption to the measurement even though they were very few in the secondary beam. An aluminum absorber in thickness of 45.9 mg/cm^2 was used for the sake of eliminating the ^{6}Li^{2+} as well as ^{7}Li ions in the secondary beam thoroughly. In the meantime the absorber degraded the ^{6}He energy down to 25 MeV. The beam was then collimated by an aperture in diameter of 3 mm and directed onto a secondary target placed on the focal plane. A polyethylene $(CH_2)_n$ foil of 1.5 mg/cm^2 thick served as the secondary target to study the reaction of interest, and a carbon foil of 1.8 mg/cm^2 thick was used to measure the background. The reaction products were detected and identified using a ΔE–E counter telescope consisting of a 19.3 μm thick silicon ΔE detector and a 45×45 mm^2 Hamamatsu X–Y sensitive silicon detector (PSSD) in thickness of 300 μm. The PSSD enabled us to determine both the remaining energy and emission angles of the outgoing ions. The inverse kinematics of the ^{1}H(^{6}He, ^{6}Li)n reaction restricted the maximum emission angle of ^{6}Li ions to about 12.8°. The setup shown in Fig. 1 covered an angular region up to 14°, thus the full angular distribution can be measured. The overall angular resolution was about 2° FWHM, which mainly resulted from the ^{6}He angular straggling in passing through the aluminum absorber.

The experimental setup also facilitated to determinate the accumulated ^{6}He events precisely because the ^{6}He themselves were recorded by the counter telescope simultaneously. However, it brought about a problem of pulse pileup. In order to solve the problem, the beam intensity on the target was kept at a very low level of 300–500 cps and the pulse pileup rejection trigger was used. The measurement for the $(CH_2)_n$ target accumulated approximately 1.38×10^8 ^{6}He events, while the background measurement with the carbon target about 6.53×10^7 ^{6}He events.

The scatter plot of ΔE vs. E (remaining energy) from a few runs with the $(CH_2)_n$ target is shown in Fig. 2. For the sake of saving CPU time, we set a cut at $\Delta E = 1.8$ MeV using software, all the events below the cut were scaled down by a factor of 100. The scatter plot of E_t vs. $\theta_{\rm lab}$ for all the ^{6}Li events within two dimension gate in Fig. 2 is shown in the bottom panel of Fig. 3, where E_t is the total energy and $\theta_{\rm lab}$ denotes the laboratory emission angle converted from the position data of PSSD. According to Monte Carlo simulation with the reaction kinematics and experimental setup, the events were identified as two groups which corresponding to the ground and 3.563 MeV 0^+ states of ^{6}Li, respectively. The projection onto the energy axis for the ^{6}Li events of $\theta_{\rm lab} < 5°$ is shown in the top panel of Fig. 3. A well separation between the ground

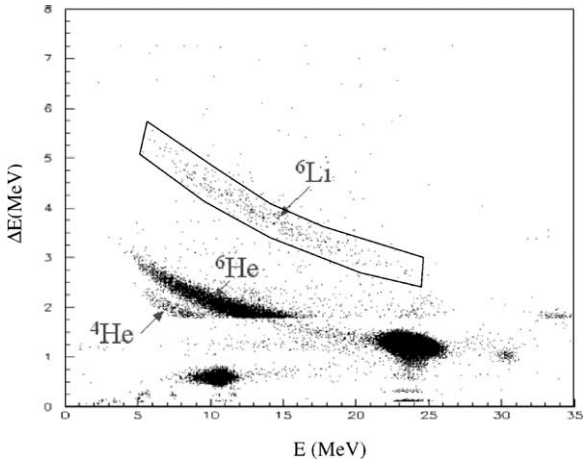

Fig. 2. Scatter plot of ΔE vs. E.

and 3.563 MeV 0^+ states of ^{6}Li can be seen. In the region of $\theta_{\rm lab} > 5°$, however, the events of two states can only be identified with the scatter plot of E_t vs. $\theta_{\rm lab}$ due to the overlap of their projections onto either the energy or angle axis.

The angular distributions are shown in Fig. 4. The open circles and filled circles are the differential cross sections with the ^{6}Li formed in its ground and 3.563 MeV 0^+ states, respectively. In the case of $\theta_{\rm lab} > 5°$, two states are not well separated, and thus a correction for their mutual contributions was carried out appropriately. The errors of cross sections are due to both the statistical uncertainties and the additional ones from the above correction. As can clearly be seen from Fig. 4, the cross section leading to the 3.563 MeV 0^+ state of ^{6}Li is obviously larger than that to the ground state around $\theta_{\rm c.m.} = 90°$. The poor angular resolution is due to the enlargement of the emission angle uncertainties in the transformation from laboratory frame to center of mass frame. The lines are the conventional DWBA calculations with the zero-range approximation by the code KORP [9] in which the microscopic optical potentials were adopted. The code has been successfully applied to the low energy (n, p) and (p, n) reactions [9,10]. The experimental angular distributions were fairly reproduced for both the ground and 3.563 MeV 0^+ states by the calculations.

In the calculation of microscopic optical potentials, the first and second order mass operators in nuclear matter were derived with Skyrme effective interactions

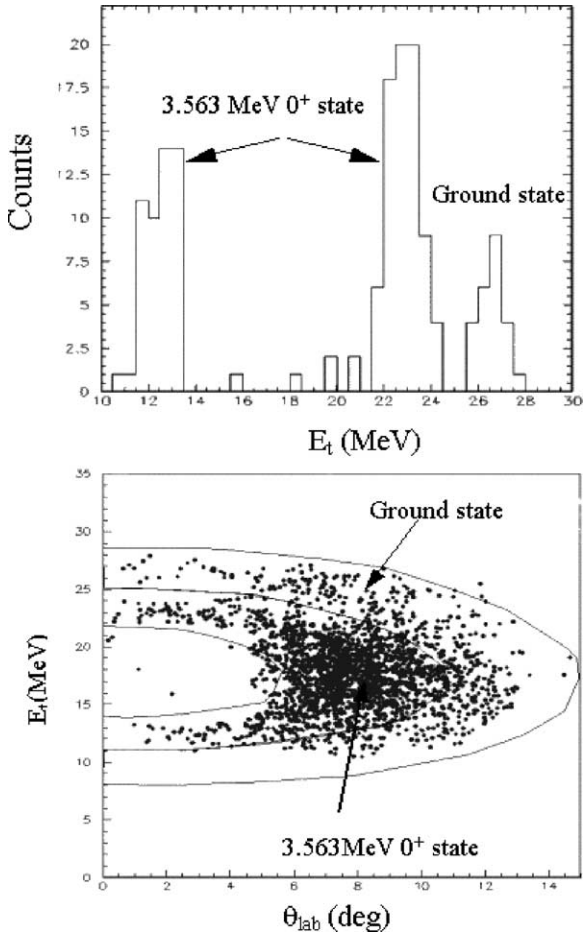

Fig. 3. Bottom panel: scatter plot of E_t vs. $\theta_{\rm lab}$ for ^{6}Li events. Top panel: a projection for ^{6}Li events of $\theta_{\rm lab} < 5°$ onto the energy axis. The left and middle peaks correspond to the 3.563 MeV 0^+ state, the angular ranges are $150° < \theta_{\rm c.m.} < 180°$ and $0° < \theta_{\rm c.m.} < 40°$, respectively. The right peak corresponds to the ground state, $\theta_{\rm c.m.} < 27°$. The ground state events of $\theta_{\rm c.m.} > 160°$ are rejected by the threshold of ΔE–E counter.

and the real and imaginary parts of the optical potential for finite nuclei were obtained by applying a local density approximation [11]. The proton and neutron density distributions of the 3.563 MeV 0^+ state of ^{6}Li and the ground state of ^{6}He used in the calculations are shown in Fig. 5. As to the ^{6}Li ground state, the density distributions for both neutron and proton are assumed to be the same as the charge density distribution in Ref. [12].

Fig. 6 shows the angular distributions of the 3.563 MeV 0^+ state of ^{6}Li calculated with different

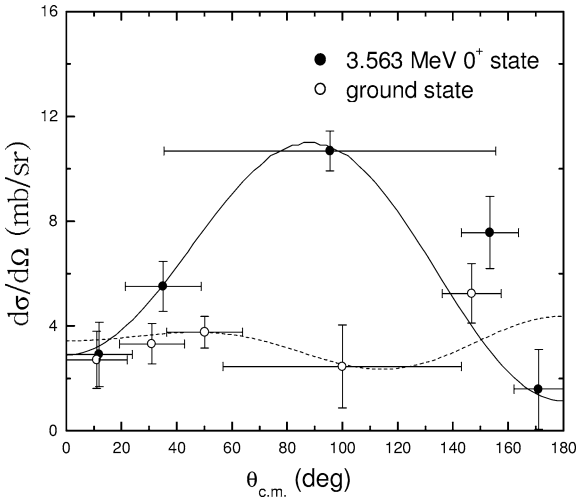

Fig. 4. Angular distributions of ^{1}H(^{6}He, ^{6}Li)n reactions.

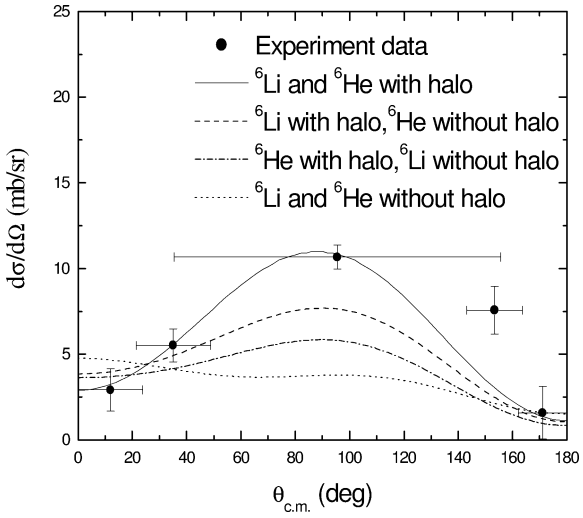

Fig. 6. DWBA calculations by different nucleon density distributions.

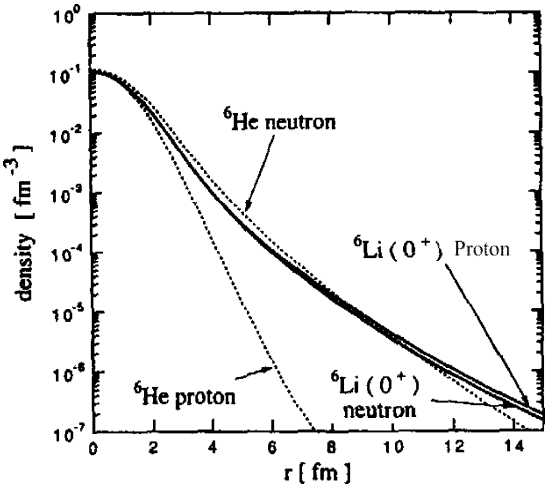

Fig. 5. Neutron and proton density distributions for the 3.563 MeV 0^{+} state of ^{6}Li and the ground state of ^{6}He used in the calculation of microscopic optical potentials. This figure is taken from Ref. [2].

nucleon density distributions. The dotted line results from the assumption of both 3.563 MeV 0^{+} state of ^{6}Li and the ground state of ^{6}He without halo, i.e., the density distribution of the former is the same as that of the ground state of ^{6}Li; and for the ground state of ^{6}He, the density distribution of neutron is similar to that of proton. The dashed-dotted line is the case of ^{6}He with neutron halo and ^{6}Li without halo. The dashed line stands for the situation of ^{6}Li with neutron–proton halo and ^{6}He without halo. The solid line refers to the calculation in which both ^{6}Li and ^{6}He are assumed to have halo structure with nucleon density distributions as shown in Fig. 5. The comparison of the calculations with different nucleon density distributions bears out the existence of both the neutron–proton halo structure for the 3.563 MeV 0^{+} state in ^{6}Li and the neutron halo structure for ^{6}He ground state.

In summary, the angular distributions of ^{1}H(^{6}He, ^{6}Li)n reaction connecting the ground state of ^{6}He and the ground and 3.563 MeV 0^{+} states of ^{6}Li have been measured using the secondary ^{6}He beam at energy of 4.17 A MeV. The experimental data can be well reproduced with the microscopic DWBA analysis if it is assumed that both the ground state of ^{6}He and the secondary excited state of ^{6}Li have halo structure. The present work reveals the proton–neutron halo structure of the secondary excited state of ^{6}Li predicted by Arai et al. [2] for the first time.

Acknowledgements

The authors would like to thank Drs. Q. Shen and C. Lin for their help in the theoretical analysis. This work was funded by the Major State Basic Research Development Program under Grant No. G200077400 and the National Natural Science Foundation of China

under Grant Nos. 19735010, 19935030, 10025524 and 10045002.

References

[1] Y. Suzuki, K. Yabana, Phys. Lett. B 272 (1991) 173.
[2] K. Arai, Y. Suzuki, K. Varga, Phys. Rev. C 51 (1995) 2488.
[3] M.D. Cortina-Gil et al., Phys. Lett. B 371 (1996) 14.
[4] J.A. Brown et al., Phys. Rev. C 54 (1996) R2150.
[5] M.D. Cortina-Gil et al., Nucl. Phys. A 616 (1997) 215c.
[6] M.D. Cortina-Gil et al., Nucl. Phys. A 641 (1998) 263.
[7] X. Bai et al., Nucl. Phys. A 588 (1995) 273c.
[8] W. Liu et al., Phys. Rev. Lett. 77 (1996) 611;
W. Liu et al., Nucl. Phys. A 616 (1997) 131c.
[9] Z. Yu, Y. Zuo, CNIC-00736, NKU-0002 (1993).
[10] Q. Shen, J. Zhang, Phys. Rev. C 50 (1994) 2473.
[11] Q. Shen et al., Z. Phys. A 303 (1981) 69.
[12] G.C. Li, I. Sick, R.R. Whitney, M.R. Yearian, Nucl. Phys. A 162 (1971) 583.